A Porous-Medium Theory for Barotropic Flow through Ridges and Archipelagos[*]

Larry J. Pratt and Michael A. Spall

Woods Hole Oceanographic Institution, Woods Hole, Massachusetts

ABSTRACT

A linear theory for the treatment of complex ridges and archipelagos as porous media is presented. The theory assumes a barotropic, wind-driven ocean with uniform depth. A porous ridge is formed by shrinking the meridional dimensions of the islands and straits (or gaps) composing a meridionally aligned island chain to infinitesimal values. The circulation integrals associated with a generalization of the "island rule" for each island then combine to form an ordinary differential equation. The solution determines the magnitude and structure of the zonal flow through the ridge. This solution could supply a boundary condition for numerical or inverse models that cannot resolve the topographic details of the ridge or archipelago. The physics of the throughflow is explored using a series of examples. It is shown that a concentrated zonal flow approaching the ridge from the east tends to spread meridionally before it passes through the ridge. If the spreading distance, which depends on the characteristics of the ridge, is small in comparison with the meridional scale of the zonal flow, the flow is unimpeded by the ridge. Otherwise the ridge may block or divert the flow. Paradoxically, ridges with high porosity are just as effective at blocking as are ridges with low porosity. The theoretical results are verified to a large extent by a barotropic numerical model.

1. Introduction

The Mid-Atlantic Ridge is a topographically complex collection of bumps and gaps that partially obstructs deep and intermediate zonal flows. A horizontal slice through the ridge at 3500-m depth (Fig. 1) reveals its geometric complexity and points out the difficulty in properly resolving it in circulation models. The Central Indian Ridge, the Ninety East Ridge, the East Pacific Rise, the Indonesian Archipelago, and the Leeward and Windward Islands are other examples of oceanographically important boundaries that impede but do not necessarily block incident currents. An obvious but unrealized alternative to resolving the topographic details of these features would be to treat them as smooth, porous boundaries. The ability of fluid to leak through would have to be tied to the geometrical properties of the ridge or archipelago, such as the percentage of the topography occupied by gaps to the lengths of the gaps and coefficients of friction. Until now, no rational, dynamically consistent way of making this connection has been suggested. The purpose of this paper is to explore the dynamical implications of such topographic features and offer a possible approach.

Our ideas will be introduced within the context of a simple, barotropic model in which the ridge extends to the surface and all sidewalls are vertical. In this setting the ridge is really an island chain or archipelago. Since many of the ridges mentioned above run north and south, we choose a meridionally aligned series of islands (Fig. 2). The islands are elongated in the zonal direction and are separated by straits, a choice motivated by the orientation of the fracture zones in Fig. 1. The lengths and widths of the gaps and islands may vary. The circulation in the vicinity of the ridge is assumed to be linear and to be forced by the wind through an Ekman pumping velocity. The main problem is to determine the extent to which the archipelago impedes any impinging Sverdrup flow. We also discuss the case of ridge-induced circulation within a layered, quasigeostrophic system.

The basic theory for the flow in the gaps is based on circulation integrals and, in particular, on a frictionally modified version of the "island rule" introduced by Godfrey (1989). When written down for a chain of islands, the circulation integrals form a set of difference equations that converge to an ordinary differential equation in the limit of infinitesimal gap and island widths. The solution to this equation gives the total meridional transport to the east of the ridge. The flow through the porous ridge is given by the divergence of this transport. The coefficients in the equation depend on the local

Corresponding author address: Dr. Larry Pratt, Woods Hole Oceanographic Institution, Mail Stop 21, 360 Woods Hole Rd., Woods Hole, MA 02543.
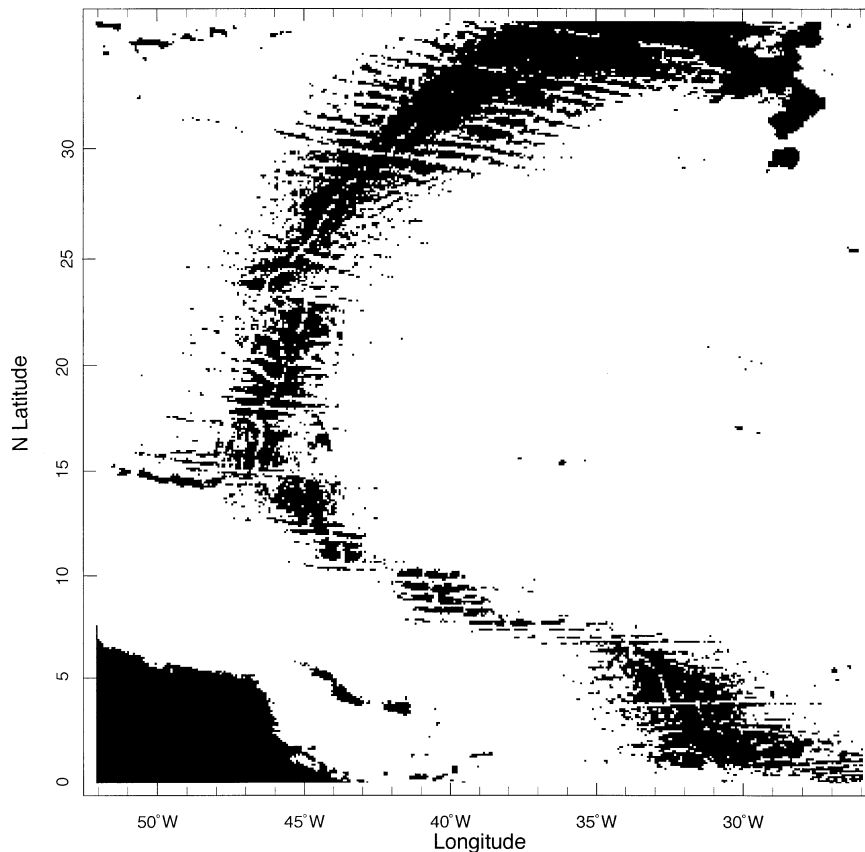E-mail: lpratt@whoi.edu

FIG. 1. A slice through the Mid-Atlantic Ridge at 3500-m depth. The shaded areas represent all shallower topography. The figure is based on the Smith and Sandwell (1997) topography.

length of the ridge and its porosity, both of which are smooth functions of the meridional variable y. The circulation integrals assume that the infinitesimal islands do not occupy common latitude bands and therefore the theory is not applicable to zonally aligned barriers such as the Indonesian Archipelago. Wajsowicz (1993a,b; 2002) has discussed extensions of the island rule to cases in which the islands overlap zonally.

The underlying physics of the theory is based on ideas involving circulation and vorticity. Flow in the infinitesimal straits is retarded by bottom friction, and this introduces a source of circulation along the integration paths where they pass through the straits. Circulation sources along the same paths are also provided by the wind stress (or, in the case of an abyssal flow, by diapycnal mixing) and by meridional fluxes of planetary vorticity associated with the Sverdrup circulation to the east of the ridge. These ideas are amplified in a series of examples designed to further the reader's physical intuition and to show how the Sverdrup flow is altered by the ridge according to different factors, including variable wind stress curl and porosity. Section 2 presents the basic theory, including the development of the governing equation and its boundary conditions at the free ends of the ridge. Analytical examples are presented in

section 3 along with verifying simulations from a barotropic numerical model. Section 4 discusses the case of a quasigeostrophic layer model. We show that the field equation governing the flow through the ridge is essentially the same as in the barotropic case. Section 5 summarizes the findings.

2. Basic theory

We will consider flows governed by the linear barotropic shallow water equations:

$$\frac{\partial \mathbf{u}}{\partial t} + f\mathbf{k} \times \mathbf{u} = -\boldsymbol{\nabla}\left(\frac{p}{\rho}\right) + \text{diss}(\mathbf{u}) + \frac{\boldsymbol{\tau}}{\rho H} \quad \text{and} \quad (2.1)$$

$$\boldsymbol{\nabla} \cdot (\mathbf{u}H) = 0, \tag{2.2}$$

with $f = f_o + \beta y$ and otherwise standard notation. The depth H is considered constant. For the present it will be assumed that the dissipation is entirely due to bottom friction parameterized as

$$\text{diss}(\mathbf{u}) = -\frac{D_f \mathbf{u}}{H}, \tag{2.3}$$
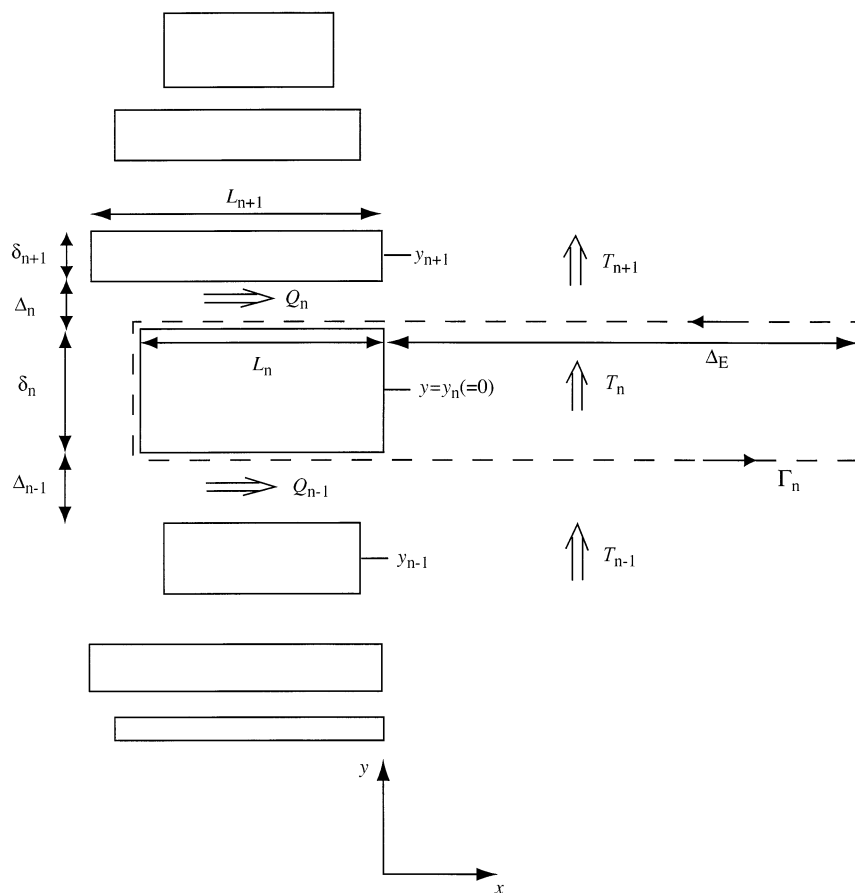
where D_f is a drag coefficient.

FIG. 2. Definition sketch showing hypothetical island chain or ridge. The T and Q represent volume transports.

Consider a meridional archipelago or ridge consisting of rectangular islands of variable size separated by straits of variable width (Fig. 2). Integration of the tangential component of (2.1) counterclockwise about the contour Γ_n and use of (2.2) and (2.3) yields

$$\frac{\partial}{\partial t} \oint_{\Gamma_n} H\mathbf{u} \cdot \mathbf{t} \, ds + \beta \delta_n T_n$$

$$= \oint_{\Gamma_n} \frac{\boldsymbol{\tau}}{\rho} \cdot \mathbf{t} \, ds - D_f \oint_{\Gamma_n} \mathbf{u} \cdot \mathbf{t} \, ds, \qquad (2.4)$$

where $\mathbf{t}$ and $\mathbf{n}$ are unit tangent and normal vectors to Γ_n, δ_n is the meridional thickness of the island, and T_n is the total meridional transport between the island and the eastern basin boundary. If the flow is steady and dissipation is negligible, the transport is given by the "island rule" (Godfrey 1989):

$$T_n = \frac{\displaystyle\int_{\Gamma_n} \frac{\boldsymbol{\tau}}{\rho} \cdot \mathbf{t} \, ds}{\beta \delta_N}. \qquad (2.5)$$

If the straits to the north and south of the island are narrow, dissipation may not be negligible where Γ_n runs through them. With free-slip conditions along the walls the zonal velocity in each strait will become uniform as its width Δ_n is reduced to zero. In this case, the contribution to the dissipation integral in (2.4) is

$$D_f L_n (u_{n-1} - u_n) = \frac{D_f L_n}{H}\left(\frac{Q_{n-1}}{\Delta_{n-1}} - \frac{Q_n}{\Delta_n}\right),$$

where Q_n is the transport in the nth strait. In many cases, the above expression will represent the predominant contribution of friction about the entire contour Γ_n. For example, the zonal velocity in the straits may be much larger than that in the interior. Or, the value of the drag coefficient D_f may be substantially greater than in the interior. An example of the latter occurs when the layer in question is imagined to be detached from the bottom away from the archipelago, as might be the case for a deep layer in the Atlantic Ocean that contacts the bottom only at the Mid-Atlantic Ridge. The dynamics of such a layer are clearly not barotropic, but the physical setting

provides ample motivation for considering a locally enhanced value of D_f.

Since, by continuity, $Q_n = T_{n+1} - T_n$, it is possible to rewrite the dissipation integral as

$$D_f \oint_{\Gamma_N} \mathbf{u} \cdot \mathbf{t} \, ds \cong \frac{D_f L_n}{H} \left(\frac{Q_{n-1}}{\Delta_{n-1}} - \frac{Q_n}{\Delta_n} \right)$$

$$= -\frac{D_f L_n}{H} \left(\frac{T_{n+1} - T_n}{\Delta_n} - \frac{T_n - T_{n-1}}{\Delta_{n-1}} \right),$$

(2.6)

and substitution into the steady version of (2.4) leads, after some rearrangement, to

$$T_{n+1} = \left(1 + \frac{\beta \delta_n H \Delta_n}{D_f L_n} + \frac{\Delta_n}{\Delta_{n-1}} \right) T_n - \frac{\Delta_n}{\Delta_{n-1}} T_{n-1}$$

$$- \frac{H \Delta_n}{D_f L_n} \oint_{\Gamma_n} \frac{\tau}{\rho} \cdot \mathbf{t} \, ds.$$

(2.7)

One could iterate this map to find all T_n provided that two consecutive values are known. In cases in which the geometric parameters δ_n, Δ_n, and L_n vary abruptly (and perhaps even randomly) with n, this is the approach that must be used to find the transports and, from them, the fluxes through the gaps. Alternatively, one could assume that the geometry, and along with it the transport T_n, vary gradually from one island to the next. Reducing δ_n and Δ_n then leads to a differential form of the map, as we now show.

Define a continuous transport function $T(y)$ that takes on the values T_j at the discrete values $y = y_j$ corresponding to the central latitudes of the islands. It is further assumed that T_j and y_j vary sufficiently gradually so that $T(y)$ has smooth first and second derivatives. A continuous $L(y)$ can be defined similarly. Then, the differences between neighboring T_i are related to the first derivative of $T(y)$ by

$$\left(\frac{dT}{dy} \right)_{y_{n+1/2}} \cong \frac{T_{n+1} - T_n}{\frac{1}{2}(\delta_n + \delta_{n+1}) + \Delta_n} \quad \text{and} \quad (2.8a)$$

$$\left(\frac{dT}{dy} \right)_{y_{n-1/2}} \cong \frac{T_n - T_{n-1}}{\frac{1}{2}(\delta_n + \delta_{n-1}) + \Delta_{n-1}}, \quad (2.8b)$$

where $y_{n+1/2} = \frac{1}{2}[\frac{1}{2}(\delta_n + \delta_{n+1}) + \Delta_n]$ and $y_{n-1/2} = \frac{1}{2}[\frac{1}{2}(\delta_n + \delta_{n-1}) + \Delta_{n-1}]$ are the midpoints between y_n and y_{n+1} and between y_n and y_{n-1}. Substitution into (2.6) leads to the estimate

$$D_f \oint_{\Gamma_n} \mathbf{u} \cdot \mathbf{t} \, ds$$

$$\cong -\frac{D_f L(y)}{H} \left[\frac{\frac{1}{2}(\delta_n + \delta_{n+1}) + \Delta_n}{\Delta_n} \left(\frac{dT}{dy} \right)_{y_{n+1/2}} \right.$$

$$\left. - \frac{\frac{1}{2}(\delta_n + \delta_{n-1}) + \Delta_{n-1}}{\Delta_{n-1}} \left(\frac{dT}{dy} \right)_{y_{n-1/2}} \right].$$

Next define the porosity function $p(y)$ to fit through the values of $\Delta_j/[\frac{1}{2}(\delta_j + \delta_{j+1}) + \Delta_j]$ at the midlatitudes $y_{j+1/2}$. Note that $p(y)$ is the local percentage of ridge meridional coastline occupied by gaps. Thus

$$D_f \oint_{\Gamma_n} \mathbf{u} \cdot \mathbf{t} \, ds$$

$$\cong -\frac{D_f L(y_n)}{H} \left\{ \left[\frac{1}{p(y)} \frac{dT}{dy} \right]_{y_{n+1/2}} - \left[\frac{1}{p(y)} \frac{dT}{dy} \right]_{y_{n-1/2}} \right\}$$

$$= -\frac{D_f L(y_n)}{H} \left\{ \left[\frac{1}{p(y)} \frac{dT}{dy} \right]_{\delta_n/2} - \left[\frac{1}{p(y)} \frac{dT}{dy} \right]_{-\delta_n/2} \right.$$

$$+ \left(y_{n+1/2} - \frac{1}{2}\delta_n \right) \left[\frac{d}{dy} \frac{1}{p(y)} \frac{dT}{dy} \right]_{\delta_n/2}$$

$$\left. - \left(y_{n-1/2} + \frac{1}{2}\delta_n \right) \left[\frac{d}{dy} \frac{1}{p(y)} \frac{dT}{dy} \right]_{-\delta_n/2} \right\}.$$

The second step involves the approximation through Taylor expansion of the values of

$$\left[\frac{1}{p(y)} \frac{dT}{dy} \right]_{y_{n\pm1/2}}$$

at $y = \pm\delta_n$ in terms of its values at the edges $y = y_{n+1/2}$.)

Shrinking the δ and Δ to zero while maintaining their relative proportions leads to

$$D_f \oint_{\Gamma_n} \mathbf{u} \cdot \mathbf{t} \, ds = -\frac{D_f L(y)}{H[1 - p(y)]} \frac{d}{dy} \left[\frac{1}{p(y)} \frac{dT}{dy} \right] \delta_n$$

$$+ O(\delta_n^2).$$

(2.9)

If the steady version of (2.4) is now divided by δ_n, the limit $\delta_n \to 0$ is taken, and (2.5) and (2.9) are used, one obtains[1]

---

[1] If the straits (rather than the islands) are each perfectly rectangular, then it can be shown that (2.10) is replaced by

$$\frac{d}{dy} \left[\frac{L(y)}{p(y)} \frac{dT}{dy} \right] - \frac{[1 - p(y)]}{\delta_s} T = -\frac{[1 - p(y)]}{\delta_s} T_1(y). \quad (2.10a)$$

$$\frac{d}{dy}\left[\frac{1}{p(y)}\frac{dT}{dy}\right] - \frac{[1 - p(y)]}{\delta_S L(y)}T = -\frac{[1 - p(y)]}{\delta_S L(y)}T_1(y),$$

$$\text{(2.10)}$$

where $\delta_S = D_f/(\beta H)$ is the characteristic thickness of a standard Stommel western boundary layer and

$$T_1(y) = \lim_{\delta_n \to 0} \frac{\oint_{\Gamma_n}(\boldsymbol{\tau}/\rho)\cdot\mathbf{t}\,ds}{\beta\delta_n} \qquad \text{(2.11a)}$$

is the transport to the east of an individual island predicted by the original island rule. If the wind stress curl varies only with y, which is assumed henceforth, then

$$T_1(y) = -\frac{L(y) + \Delta_E(y)}{\beta}\frac{\partial}{\partial y}\left[\frac{\tau^{(x)}}{\rho}\right], \qquad \text{(2.11b)}$$

where Δ_E is the distance from the east coast of the porous ridge to the eastern basin boundary. Note that T_1 is just the total Sverdrup transport across the line extending from the position of the west edge of the ridge to the eastern basin boundary (and assuming the ridge was absent).

Any divergence in $T(y)$ implies a flow through the porous ridge. The velocity

$$u_R(y) = \frac{1}{H}\frac{\partial T}{\partial y} \qquad \text{(2.12)}$$

is the zonal velocity through the ridge averaged over a small interval in y that includes both gaps and solid material. This velocity also provides a boundary condition on the flow to the west of the ridge. The actual velocity in the infinitesimally thin straits [equivalent to the u arising in (2.6)] is given by u_R/p. One measure of the effect of the ridge is the difference between u_R and the zonal velocity that would occur in the absence of the ridge. The latter is just the zonal Sverdrup velocity u_s evaluated, say, at the west edge ($x = -L$) of the ridge:

$$u_S(-L, y) = \frac{1}{\beta H}\int_{-L}^{\Delta_E}\frac{\partial}{\partial y}\,\text{curl}\left(\frac{\tau}{\rho}\right)dx. \qquad \text{(2.13)}$$

Equation (2.10) governs the y variation of transport to the east of the porous ridge. For the case of constant L and p, such variations clearly involve the length scale

$$l = \frac{(\delta_S L)^{1/2}}{p^{1/2}(1 - p)^{1/2}}, \qquad \text{(2.14)}$$

which is proportional to the characteristic thickness $(\delta_S L)^{1/2}$ of the diffusive boundary layer that occurs along meridional boundaries in a Stommel circulation model (Pedlosky 1968 and also see Faller 1960). It will be shown that l is the meridional distance that an isolated band of impinging zonal flow must spread before it can pass through the ridge. Note that l is quite large for a relatively impermeable ridge ($p \ll 1$) as well as a highly

porous ridge ($p \gg 1$). The former case is no surprise: a nearly solid ridge should spread disturbances out over very large meridional distances. The latter case is less intuitive: one might think that a highly porous ridge would allow the flow to pass through with little meridional spreading. A careful examination of the steady version of the circulation integral (2.4) for an individual island shows that the real situation is more complicated. For simplicity, assume that the strait widths and the island widths are uniform ($\delta_n = \delta$) and ($\Delta_n = \Delta$). In the limit of vanishing δ and Δ each of the terms in (2.4) tends to zero. The terms involving the transport T_n and the wind stress each go to zero in proportion to δ, meaning that the dissipation term must go to zero at the same rate. The latter is proportional to ($u_n - u_{n-1}$). Now suppose that in the limit $p \to 1$ the meridional spreading scale remains finite, implying that d^2T/dy^2 remains finite. From the previous results it can easily be shown that

$$\frac{d^2T}{dy^2} = \frac{\Delta H(u_n - u_{n-1})}{(\delta + \Delta)^2}.$$

If $\delta \ll \Delta$, which is the case for $p \to 1$, then the above relation suggests that ($u_n - u_{n-1}$) goes to zero in proportion to Δ, not δ. In other words, the dissipation about an individual island that is implied when the boundary is very porous and when the meridional spreading scale is finite is too large to balance the other terms in the circulation integral. Essentially, a finite variation in dT/dy implies an unacceptably large velocity difference between the north and south sides of the disproportionately thin island.

Suppose that the north and south tips of the archipelago, which lie at latitude y_N and y_S, are well separated from any basin boundaries or other islands. Then boundary conditions on T at $y = y_N$ and $y = y_S$ can be formulated by evaluating (2.4) around the southernmost and northernmost islands. Consider the south tip, as defined by island $n = 1$. The dissipation in the gap between the strait immediately to the north can be calculated as before, while the dissipation along the southern boundary of the island is different. As discussed by Pedlosky et al. (1997) and Pratt and Pedlosky (1998) a diffusive boundary layer whose thickness increases to the west can be expected (Fig. 3). The velocity in the boundary layer is given in appendix A and the corresponding contribution to the dissipation integral in (2.4) is[2] $2(\delta_S L_1/\pi)^{1/2}[\beta T_1 - (\frac{2}{3}L_1 + \Delta_E)\,\text{curl}(\tau/\rho)_{y_S}]$. With these representations of dissipation, the steady form of (2.4) becomes

$$-\beta\delta_1 T_1 = -\oint_{\Gamma_1}\frac{\tau}{\rho}\cdot\mathbf{t}\,ds + -\frac{D_f L_1}{\Delta_1 H}(T_2 - T_1)$$

$$+ 2\left(\frac{\delta_S L_1}{\pi}\right)^{1/2}\left[\beta T_1 - \left(\frac{2}{3}L_1 + \Delta_E\right)\text{curl}\left(\frac{\tau}{\rho}\right)_{y_1}\right].$$

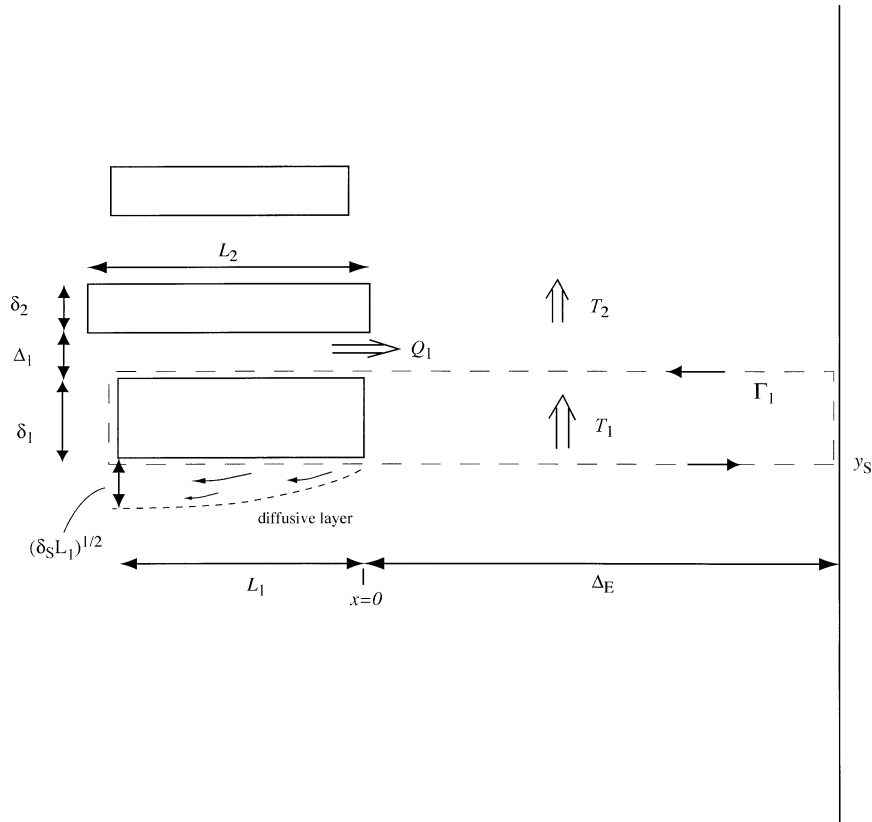
[2] See, for example, Eq. (A.5) of Pratt and Pedlosky (1998).

Fig. 3. Definition sketch for the diffusive boundary layer on the south face of the southernmost island in the chain.

In the limit $\delta_1 \to 0$ (and $\Delta_1 \to 0$), the first two terms vanish, while the third can be related to the derivative of T using (2.8). The remaining balance of terms requires that the net dissipation (and therefore the net tangential velocity) about the southern island be zero. After a bit of further manipulation this requirement can be written as

$$\frac{\partial T}{\partial y} = 2\frac{p}{(\delta_S L \pi)^{1/2}}\left[T - \frac{\frac{2}{3}L + \Delta_E}{\beta}\,\mathrm{curl}\!\left(\frac{\boldsymbol{\tau}}{\rho}\right)\right] \quad (y = y_S).$$
(2.15a)

A similar calculation about the island forming the northern tip of the ridge yields

$$\frac{\partial T}{\partial y} = -2\frac{p}{(\delta_S L \pi)^{1/2}}\left[T - \frac{\frac{2}{3}L + \Delta_E}{\beta}\,\mathrm{curl}\!\left(\frac{\boldsymbol{\tau}}{\rho}\right)\right] \quad (y = y_N).$$
(2.15b)

3. Examples

We now present some simple examples designed to provide insight into the influence of a porous ridge upon a flow that is otherwise controlled by Sverdrup dynam-

ics. It will be useful to compare the porous ridge solutions with the flow that would occur if the ridge were solid. In this case the meridional transport T_R to the east of the ridge would be constant and would in many settings be well approximated by the original island rule[3] for the ridge as a whole. The correct formula is obtained by replacing Γ_n in (2.5) with Γ_R, the contour circling the area occupied by the ridge plus the area to the east of the ridge. Thus

$$T_R \cong \frac{\oint_{\Gamma_R}(\boldsymbol{\tau}/\rho)\cdot \mathbf{t}\,ds}{\beta(y_N - y_S)} = \frac{1}{y_n - y_S}\int_{y_S}^{y_N} T_I(y)\,dy. \quad (3.1)$$

The final expression shows that T_R is just the meridional average over the latitude band of the ridge of the total Sverdrup transport $T_I(y)$ between the west edge of the ridge and the eastern basin boundary (if one ima-

---

[3] Pedlosky et al. (1997) tested the island rule in barotropic simulations of wind driven flow around islands of different sizes and shapes. One of the few cases of failure of the physical assumptions underlying the island rule occurs when the meridional dimension of the island is much smaller than its zonal dimension. In this case the transport to the east of the island can still be predicted using a modified formula. The original island rule remains robust for other shapes, provided the island is well separated from basin boundaries.

gines that the ridge is absent). It is sometimes convenient to think of T_R as being composed of two parts, the first being the meridional average of the Sverdrup transport over the area to the east of the ridge and the second being the meridional average over the footprint of the ridge. As (2.11b) shows, variations in the prespecified function T_I are due to variations in the wind stress curl or in the dimension $L + \Delta_E$. Such variations introduce divergence in the meridional Sverdrup transport, giving rise to a zonal Sverdrup velocity toward (or away from) the ridge. In the case of a solid ridge this impinging flow would be diverted into a western boundary layer on the east coast of the island. With a porous ridge, some fluid might pass directly through the ridge or be diverted into a leaky western boundary layer.

The examples will be worked out using nondimensional versions of the governing equations with

$$ L = L_o \tilde{L}(\tilde{y}), \qquad (T, T_I) = (\tilde{T}, \tilde{T}_I)/T_o, $$

$$ u = \tilde{u} T_o/H(\delta_s L_o)^{1/2}, \quad \text{and} \quad y = \tilde{y}(\delta_s L_o)^{1/2}, $$

where L_o and T_o are typical values of L and T_I. Introducing these new variables into (2.10) and its boundary conditions (2.15a,b) and dropping the tilde notation leads to

$$ \frac{d}{dy}\left[\frac{1}{p(y)}\frac{dT}{dy}\right] - \frac{[1 - p(y)]}{L(y)}T = -\frac{[1 - p(y)]}{L(y)}T_I, \quad (3.2) $$

$$ \frac{\partial T}{\partial y} = \frac{2p}{\sqrt{\pi}}[T - \alpha_S T_1] \qquad (y = y_S), \quad \text{and} \quad (3.3a) $$

$$ \frac{\partial T}{\partial \tilde{y}} = -\frac{2p}{\sqrt{\pi}}[T - \alpha_N T_1] \qquad (y = y_N), \quad (3.3b) $$

where

$$ \alpha_{N,S} = \frac{\frac{2}{3}L_{N,S} + \Delta_E}{L_{N,S} + \Delta_E} $$

and where (2.11b) has been used to write curl(τ/ρ) in terms of T_I. In most applications $(\delta_s L_o)^{1/2}$ will be much less than the meridional extent of the ridge and therefore $\tilde{y}_N - \tilde{y}_S \gg 1$ in our examples.

a. Constant wind stress curl with constant L and p

Consider the flow produced by a uniform wind stress curl (i.e., $T_I = $ const) past a ridge with constant width L and porosity p. The value of L can be set to unity with no loss of generality. With negative wind stress curl ($T_I = -1$) the uniform meridional Sverdrup velocity is southward everywhere, with some flow impinging on the north coast of the ridge (Fig. 4). Since the meridional Sverdrup transport is nondivergent, there is no zonal flow impinging on the ridge. The original island rule (3.1) for a solid ridge would require that all the impinging flow from the north be deflected east and
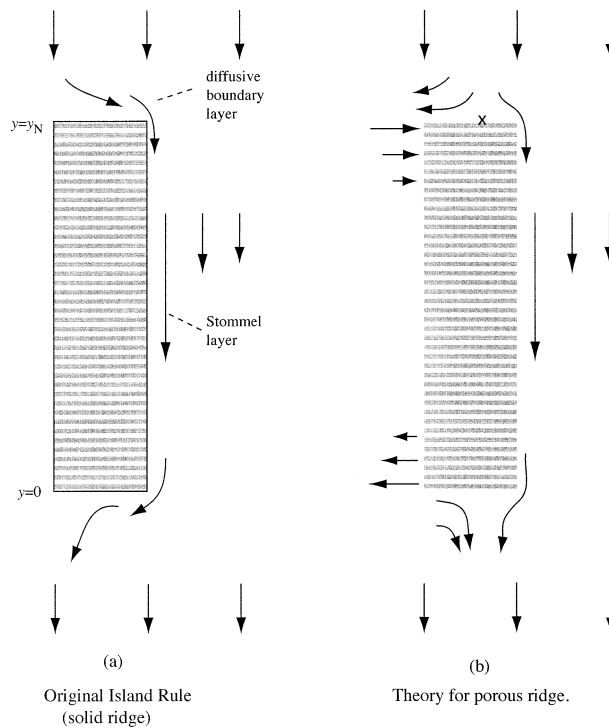

FIG. 4. Schematic diagram showing the circulation around (a) a solid ridge as opposed to (b) a porous ridge under conditions of uniform wind stress curl.

then southward past the northeast corner, where it would form a Stommel western boundary layer (Fig. 4a). The diversion of the flow would take place within a diffusive boundary layer of the type discussed above. The total transport to the east of the ridge would equal the sum of the Sverdrup transport there and the Sverdrup transport impinging on the northern boundary. The western boundary layer would eventually round the southeast corner and be reabsorbed into the Sverdrup regime to the south of the ridge.

When the ridge is porous, the situation described above occurs over the interior latitude range of the ridge (away from the northern and southern boundaries). This follows from the fact that $T(y) = T_I (= -1)$ is a solution to (3.2), though not the boundary conditions (3.3a,b). Departures from this "interior" solution occur within distance $[p(1 - p)]^{-1/2}$ of the end points $y = y_S = 0$ and $y = y_N$ of the ridge. As long as $y_N \gg [p(1 - p)]^{-1/2}$, the full solution can be approximated as

$$ T(y) = -1 + \frac{1 - \alpha}{1 + \dfrac{\sqrt{\pi}(1 - p)^{1/2}}{2p^{1/2}}} $$

$$ \times [e^{-p^{1/2}(1-p)^{1/2}y} + e^{p^{1/2}(1-p)^{1/2}(y-y_N)}] $$

$$ + O[e^{-p^{1/2}(1-p)^{1/2}y_N}]. \quad (3.4) $$

The corresponding nondimensional zonal velocity

through the ridge is given by the nondimensional version of (2.12) as

$$
u_R(y) = \frac{dT}{dy} = \frac{-(1 - \alpha)p^{1/2}(1 - p)^{1/2}}{1 + \dfrac{\sqrt{\pi}(1 - p)^{1/2}}{2p^{1/2}}}
$$
$$
\times \; [e^{-p^{1/2}(1-p)^{1/2}y} - e^{p^{1/2}(1-p)^{1/2}(y-y_N)}]
$$
$$
+ \; O[e^{-p^{1/2}(1-p)^{1/2}y_N}]. \tag{3.5}
$$

To explain the departure of the solution from the interior solution $T = T_I$ near the tips of the ridge, it is helpful to note that the situation depicted in Fig. 4 would violate the boundary condition at $y = y_N$, which requires that the net dissipation (and therefore the net zonal velocity) about the northernmost "island" be zero. The deflection of *all* of the Sverdrup transport impinging on the north face of the ridge to the east would require an eastward flow in the first gap to the south of $y = y_N$. This flow would feed into the western boundary layer on the ridge and increase its transport above the value predicted by the island rule. In reality it can be shown that the flow impinging on the northern boundary splits and flows eastward and westward about a stagnation point (marked with an X in Fig. 4b). The circulation can be calculated using the equations describing the diffusive boundary layer on the north and south coasts of the ridge (see appendix A). The average zonal velocity along the northern boundary is still eastward and an eastward gap flow is required to bring the net dissipation to zero. Eastward flows in the gaps farther to the south are also set up, and the associated transport is added to the Stommel western boundary layer, raising its transport to the required value. A similar effect occurs near $y = y_S$.

A shallow-water model has been run using a constant wind stress curl to the east of the western edge of the ridge for comparison with the theory. The ridge is composed of a series of thin but finite rectangular islands. The model equations and solution procedure are presented in appendix B. The difference in the zonal velocity at a position just to the west of the ridge and the zonal velocity at the same position but with no ridge is shown by a solid line in Fig. 5. The general character of the solution is very similar to that predicted by the linear theory[4] (dashed line in Fig. 5). The zonal velocity through the ridge is zero except near the ridge tips. Just beyond the tips, the zonal velocity is determined in theory by the solutions (appendix A) for the diffusive boundary layers that run along the north and south faces of the tips. The solutions have been used to extend the analytical velocity profile in Fig. 5 beyond the ridge tips. The results show strong, alternating zonal flows in these areas. (The extreme values of the theoretical zonal

---

[4] The shallow-water model uses a different nondimensionalization than the analytic solutions in the paper. The theory is converted into the model nondimensional scaling when they are compared directly.
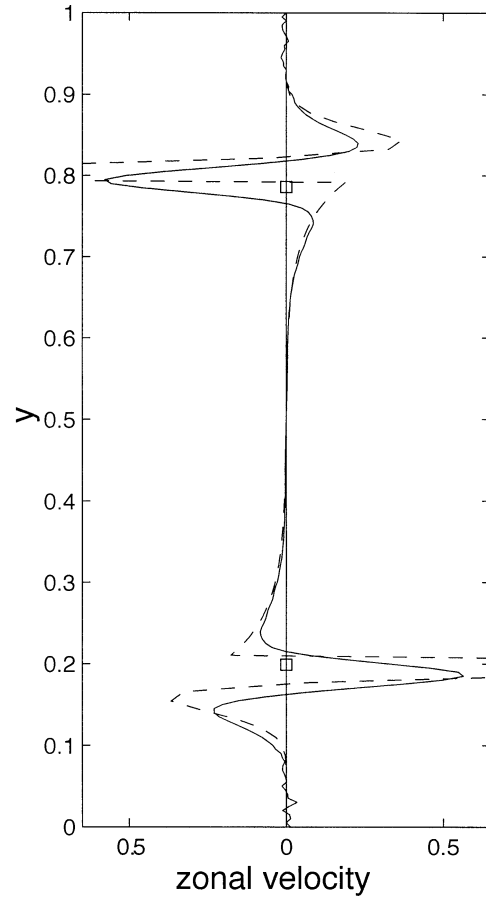

FIG. 5. The perturbation zonal velocity just to the west of a porous ridge with $p = 0.2$ according to the theory (dashed curve) as calculated by (3.5) and the numerical model (solid curve). The ridge is located between $y = 0.2$ and $y = 0.8$ (indicated on the figure by the squares). The curves have been extended to show the zonal velocity to the north and south of the ridge tips. The theoretical velocity for this case is given by the equations appearing in appendix A. The velocities have been nondimensionalized by the meridional Sverdrup velocity to the east of the ridge.

flows are approximately ± 2 and are not shown here in order to reveal the boundary layers extending along the ridge system.) These features also appear in the numerical simulation but with moderately reduced amplitude. The most likely explanation for this discrepancy is that the analytical theory predicts discontinuities in zonal velocity at $y = 0$ and $y = y_N$, a consequence of the inability of the theory to take corner effects into consideration. In reality, smoothing of the velocity profile accompanied by diminished velocity extremes should be expected, and this is what seems to occur in the numerical results.

b. Linear variation in wind stress curl with constant p and L

In the previous case, the meridional Sverdrup transport to the east of the ridge is divergence free and thus

no flow through the ridge is forced, at least away from the north and south tips. Now consider the case of a linearly varying wind stress curl:

$$T_l = -\frac{y}{y_N}. \tag{3.6}$$

The meridional Sverdrup transport to the east of the island is now divergent, implying a zonal velocity towards the ridge. The solution $T = T_l = -y/y_N$ is valid for the interior latitude range of the ridge and the corresponding flow through the ridge is given by

$$u_R = dT_l/dy = -1/y_n. \tag{3.7}$$

This value is identical to the zonal Sverdrup velocity $u_S(-L, y)$ that would exist at $x = -L$ if the ridge was absent. The zonal velocity in each infinitesimal strait u_R/p is also uniform. Although the dissipation along the north and south faces of each island is finite, the two contributions cancel in the integration around the island. Therefore the original island rule (applied about each island) continues to predict the correct transport to the east of the ridge interior. The interior ridge has no effect on the zonal velocity of the flow, even though fluid parcels passing through feel some dissipation.

The full solution for this case is given by

$$T = -\frac{y}{y_N} - \frac{1}{y_n\left[p^{1/2}(1-p)^{1/2} + \dfrac{2p}{\sqrt{\pi}}\right]}e^{-p^{1/2}(1-p)^{1/2}y}$$

$$+ \frac{y_N^{-1} + \dfrac{2p}{\sqrt{\pi}}(1-\alpha)}{p^{1/2}(1-p)^{1/2} + \dfrac{2p}{\sqrt{\pi}}}e^{p^{1/2}(1-p)^{1/2}(y-y_N)} + O(e^{-y_N}). \tag{3.8}$$

As before, departures from the solution $T = T_l$ occur only near the north and south tips (Fig. 6). Near the north tip the impinging meridional Sverdrup flow splits and flows eastward and westward about a stagnation point. The physics is similar to that discussed in connection with case (a) (Fig. 4b). At the south tip of the ridge the solution looks a little different because of the fact that the meridional Sverdrup transport at this latitude is zero.

The shallow-water model has been run using a linear variation in the wind stress curl to the east of the porous ridge for comparison with the theory. The streamfunction over the entire model domain is shown in Fig. 7. The stagnation point on the northernmost island is evident, as is the narrow southward flowing boundary layer along the eastern flank of the ridge. These perturbations to the wind-driven flow in the absence of the ridge are consistent with the schematic diagram based on the theory in Fig. 6. It is also evident from the streamline patterns in Fig. 7 that, even though the ridge is 80% solid, the zonal transport is essentially the same as would be found in the absence of the ridge.
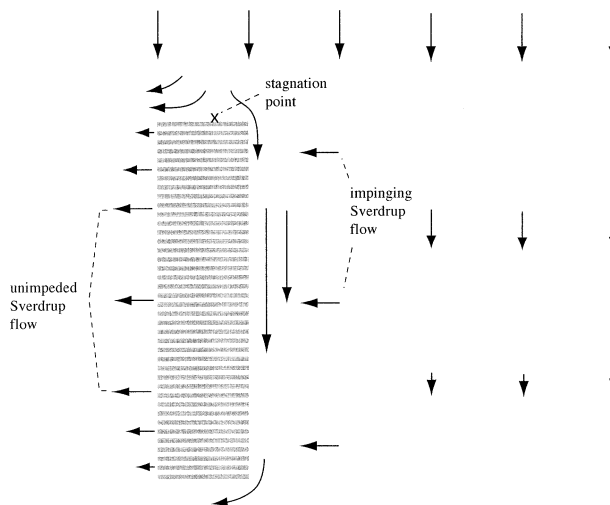

FIG. 6. Schematic representation of the theoretical circulation around a porous ridge in the presence of a wind stress curl that varies linearly in y.

The difference in the zonal velocity at the western edge of the ridge $x = 0.4$ between the case with the porous ridge and a case with no ridge is shown in Fig. 8. (solid line). The general character of the solution is very similar to that predicted by the theory (dashed line). The values have been normalized by the magnitude of the Sverdrup zonal velocity that would exist at the same location if the ridge were absent. The theoretical velocity profiles have again been extended slightly beyond the tips of the ridge using the solution for the diffusive boundary layers. As before, the perturbations are confined near the ends of the ridge, with counterflowing zonal jets just to the north and south of the islands. Meridional smoothing of the discontinuity in the zonal velocity predicted by the theory is again found in the numerical solutions.

The end effects of the ridge decay toward the middle of the ridge with meridional scale $l = [(\delta_s L)/p(1 - p)]^{1/2}$. This length scale dependency is tested in a series of numerical model runs in which the porosity p is varied between 0.1 and 0.8. In order to maintain numerical accuracy, the boundary layer width δ_s has been increased from 0.005 to 0.01 in the case of $p = 0.8$ so that the width of the gaps remains close to this boundary layer width. (The theory assumes $\Delta_n \ll \delta_s$.) In this case, the width of the ridge L has been reduced by 50% such that the product $\delta_s L$ is the same for all experiments. The meridional scale over which the perturbation in the zonal flow extends has been derived from the numerical model by calculating the meridional distance over which the eastward zonal velocity decreases to $1/e$ of its maximum value near the northern tip of the ridge. The results are shown in Fig. 9. The general trend of the influence of the north tip of the ridge extending farther southward along the ridge as the porosity decreases is reproduced well by the model. This length scale also increases for
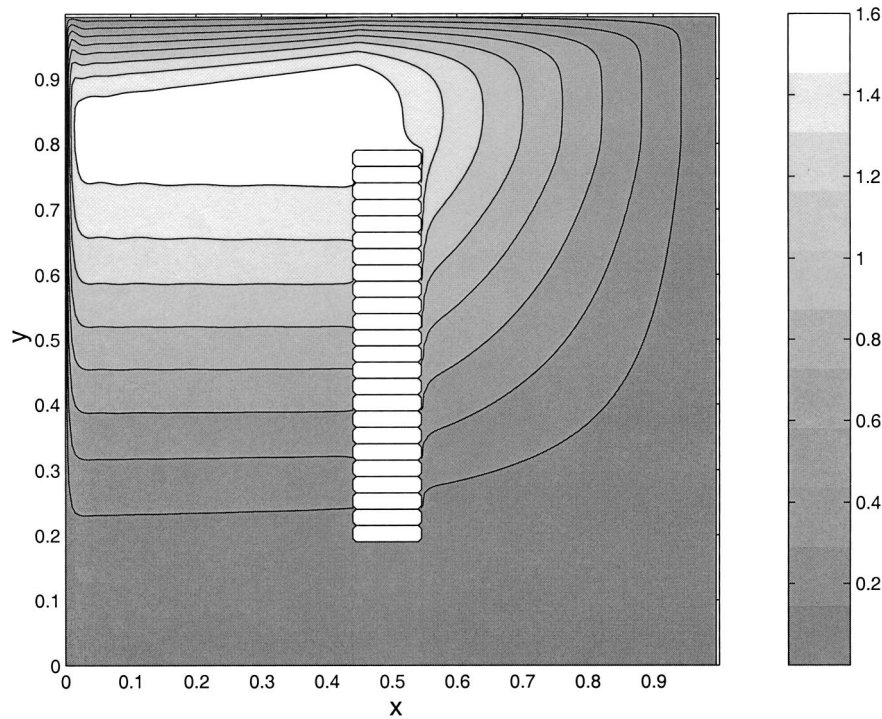
FIG. 7. Transport streamfunction from the shallow-water model for a calculation with a linear variation in the wind stress curl between the tips of the porous ridge. The individual islands composing the ridge are indicated by the white rectangles between $y = 0.2$ and $y = 0.8$.

large porosity, but it must be kept in mind that, due to numerical constraints, the assumption $\Delta_n \ll \delta_s$ is not well satisfied for this case.

c. Sinusoidal variation in wind stress curl

In the previous example the porous ridge fails to impede the zonal Sverdrup flow impinging from the east (at least away from the ridge tips). The key element is that the impinging flow is uniform with respect to y and the corresponding uniform flow in the gaps yields zero net dissipation about any infinitesimal island. The simplest way to explore departures from this picture is to consider a sinusoidal variation in wind stress curl:

$$T_I = \sin(2\pi y/\lambda). \quad (3.9)$$

For this case the zonal Sverdrup velocity produced at the position of the western edge of the ridge would, in the absence of the ridge, be

$$u_S(-L, y) = \frac{2\pi \cos(2\pi y/\lambda)}{\lambda}.$$

The interior solution to (3.2) is given by

$$T(y) = \frac{p(1-p)}{\left[\dfrac{(2\pi)^2}{\lambda^2} + p(1-p)\right]} \sin\left(\frac{2\pi y}{\lambda}\right). \quad (3.10)$$

(To this solution must be added boundary layer correc-

tions to satisfy the boundary conditions at $y = 0$ and $y = y_N$.) The corresponding zonal velocity through the ridge is given, relative to the corresponding Sverdrup velocity, by the constant factor

$$\frac{u_R(y)}{u_S(-L, y)} = \frac{1}{\left[\dfrac{(2\pi)^2}{\lambda^2 p(1-p)} + 1\right]}$$

$$= \frac{1}{\left[(2\pi)^2\left(\dfrac{l}{\lambda^*}\right)^2 + 1\right]} < 1, \quad (3.11)$$

where l is the length scale given by (2.14) and λ^* is the meridional scale of the zonal Sverdrup flow. The Sverdrup transport is impeded when the λ^* is the same order as l or smaller than l. Strong impedance tends to occur when the ridge is very nearly solid ($p \ll 1$) or the ridge is very porous ($1 - p \ll 1$). Note that the interior solution for an arbitrary $T_I(y)$ can be constructed by combining solutions of the form (3.10) as a Fourier integral over λ.

An example of the constant impedance all along the ridge interior is demonstrated using the numerical model for a case of sinusoidal wind stress curl, as in (3.9), with $(l/\lambda) = 0.15$. The zonal velocity in the model in the absence of the ridge is indicated in Fig. 10 by the dashed line. With a porous ridge, the theory predicts a reduction in the zonal velocity by a uniform factor, given
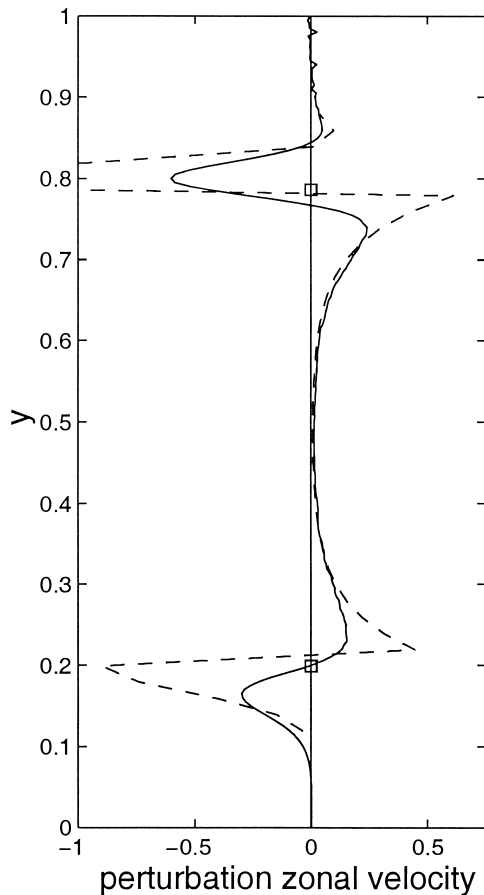
FIG. 8. Comparison between the theoretical and numerical velocity profiles measured along a position just to the west of the porous ridge under conditions simulated in Fig. 7. The dashed curve gives the difference between the theoretical zonal velocity [(3.8)] and the (constant) Sverdrup zonal velocity. The solid curve gives the same quantity based on the numerical solution. In both cases the results are normalized by the zonal Sverdrup velocity at the west edge of the ridge. The profiles have been extended beyond the north and south tips of the ridge (indicated by squares) as before.

by (3.11), of 0.53. The ratio of the zonal velocity with the ridge to the zonal velocity in the absence of the ridge from the numerical model at $x = 0.4$ is shown in Fig. 10 (the ratio is not plotted in regions where the zonal velocity is small or outside the latitude range of the ridge). The ratio is nearly uniform and reasonably close to the theoretical prediction of 0.53.

d. Isolated wind stress curl

If the Sverdrup flow impinging from the east is isolated, the effect of the ridge is to smooth out the throughflow. This behavior can be seen by considering a wind stress curl that is isolated within a latitude band $|y| < y_o$:

$$T_I = \begin{cases} -1 & (y > y_o) \\ -y/y_o & (|y| \leq y_o) \\ 1 & (y < -y_o). \end{cases} \quad (3.12)$$

In the absence of the ridge the zonal Sverdrup velocity that would occur at the position of the west edge of the ridge is $-1/y_o$ within $|y| < y_o$ and is zero otherwise (Fig. 11). If the ridge extends far to the north and south of the band $|y| < y_o$, then the solution to (3.2), which has continuous T_I and dT_I/dy across $y = \pm y_N$, is

$$T_I = \begin{cases} a \sinh[p^{1/2}(1-p)^{1/2}y_o]e^{-p^{1/2}(1-p)^{1/2}(y-y_o)} - 1 \\ \quad (y > y_o) \\ a \sinh[p^{1/2}(1-p)^{1/2}y] - y/y_o \\ \quad (|y| \leq y_o) \\ -a \sinh[p^{1/2}(1-p)^{1/2}y_o]e^{p^{1/2}(1-p)^{1/2}(y+y_o)} + 1 \\ \quad (y < -y_o), \end{cases}$$

$$(3.13)$$

where

$$a = \frac{1}{y_o p^{1/2}(1-p)^{1/2}\{\sinh[p^{1/2}(1-p)^{1/2}y_o] + \cosh[p^{1/2}(1-p)^{1/2}y_o]\}}.$$

The case of isolated wind stress curl is also well reproduced by the numerical model. The zonal velocity just to the west of the ridge is shown in Fig. 11 for both the numerical model and the theory. The wind stress curl is confined to the east of the ridge in the latitude band $y = 0.4$ to $y = 0.6$ (indicated on the figure by the dotted lines). The presence of the porous ridge spreads this zonal flow meridionally such that its influence west of the ridge can be felt across the entire latitude range of the ridge. As a result, the maximum zonal velocity is decreased to approximately 80% of that found in the

absence of the ridge. The total flux of the smoothed flow is the same as if the ridge was not present.

e. Variable $L(y)$ and $p(y)$

To this point we have treated the gap length function $L(y)$ and the porosity $p(y)$ as constant. In reality, these functions will vary about mean values, perhaps in a highly irregular way. In order to investigate the effect of such variations on the otherwise uniform flow through the porous boundary, we consider several spe-
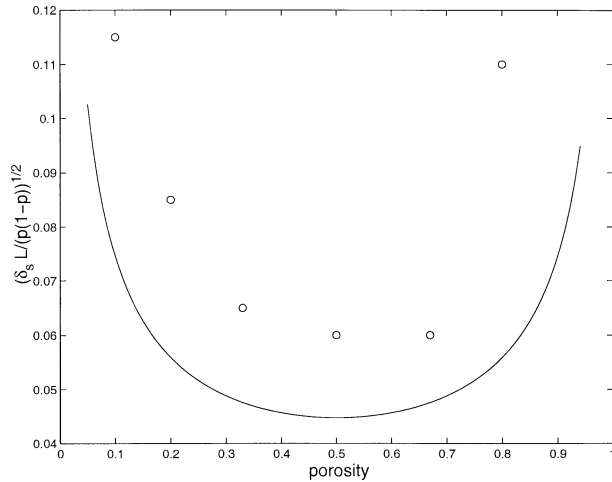
FIG. 9. Width of the boundary layer near the northern tip of the porous ridge as a function of the porosity. The solid line is $[\delta_s L/p(1-p)]^{1/2}$ from (2.14). The boundary layer widths diagnosed from a series of shallow-water model calculations in which the porosity is varied are indicated by the circles.

cial cases. We further restrict attention to the "interior" solution (away from the ends of the ridge) by making the ridge infinitely long and assume that the wind stress curl varies linearly with y: $T_I = -y$.

First note that, if p is constant, $T = T_I = -y$ is the interior solution to (3.2) for arbitrary $L(y)$. In this case the flow through the ridge is uniform and the net dissipation around each island is zero, despite the fact that the islands vary in length.

A more interesting situation occurs when L is fixed and p is allowed to vary. First consider the case in which $p(y)$ changes abruptly from one value to another:

$$p(y) = \begin{cases} \overline{p} + \delta p & (y > 0) \\ \overline{p} & (y < 0). \end{cases} \quad (3.14)$$

The interior solution is required to satisfy (3.2) away from $y = 0$, to be continuous across $y = 0$, and to satisfy the additional matching condition

$$\frac{1}{\overline{p} + \delta p}\frac{dT}{dy}\bigg|_{y=0^+} = \frac{1}{\overline{p}}\frac{dT}{dy}\bigg|_{y=0^-}, \quad (3.15)$$

obtained by integrating (3.2) across $y = 0$. The velocity through the ridge associated with the corresponding solution is given by

$$\frac{u_R(y)}{u_S(-L)} = -1 + \gamma_P \begin{cases} [-(\overline{p} + \delta p)(1 - \overline{p} - \delta p)]^{1/2} e^{-[(\overline{p}+\delta p)(1-\overline{p}-\delta p)]^{1/2}y/L} & (y > 0) \\ [\overline{p}(1 - \overline{p})]^{1/2} e^{-\overline{p}^{1/2}(1-\overline{p})^{1/2}y/L} & (y < 0), \end{cases} \quad (3.16)$$

where

$$\gamma_P = \frac{\overline{p}^{-1} - (\overline{p} + \delta p)^{-1}}{\dfrac{(1 - \overline{p})^{1/2}}{\overline{p}^{1/2}} + \dfrac{(1 - \overline{p} - \delta p)^{1/2}}{(\overline{p} + \delta p)^{1/2}}}.$$

As shown in Fig. 12a, the Sverdrup velocity through the ridge is enhanced slightly to the north of the discontinuity and retarded slightly to the south. This situation might be thought of as arising in the following way. Suppose that the zonal transport through the ridge was uniform and equal to the zonal Sverdrup transport. Then the actual westward zonal velocity u_R/p in each strait would be greater in the south than to the north owing to the fact that the porosity (and therefore the relative width of each infinitesimal strait) is lower there. This situation would yield a net negative circulation and therefore a net negative dissipation around the island centered at $y = 0$. According to (2.4) this dissipation would give rise to a northward anomaly in the transport T to the east of the ridge. This transport would pass through and add to the zonal Sverdrup transport to the north of $y = 0$, while the zonal transport to the south would be diminished. As suggested in Fig. 12a, something close to this occurs. Note that the discontinuity in

u_R becomes smoothed in the u_R/p field (Fig. 12b). In fact, the matching condition (3.15) is simply a statement of continuity of this velocity component. It is also interesting to note that the westward strait velocity is actually *weaker* in the north than the south.

If the porosity varies rapidly in y about some mean value $\overline{p}$, then the last example suggests that the throughflow should consist of variations in y about the zonal Sverdrup velocity. Let

$$p = \overline{p} + \varepsilon\hat{p}(y/\varepsilon), \quad (3.17)$$

with $\varepsilon \ll 1$ so that (3.2) becomes

$$\frac{d^2T}{dy^2} - \frac{\hat{p}'}{\overline{p} + \varepsilon\hat{p}}\frac{dT}{dy} - \frac{(\overline{p} + \varepsilon\hat{p})(1 - \overline{p} - \varepsilon\hat{p})}{L}$$
$$\times (T - T_I) = 0. \quad (3.18)$$

A numerical solution to (3.18) for the case $T_I = -y/y_N$, $\overline{p} = 0.5$, $\hat{p} = a\sin(y/\varepsilon)$, $\varepsilon = 0.2$, and $y_N = 20$ (solid curve in Fig. 13) shows that u_R contains rapid fluctuations on the same scale of the fluctuations of the porosity. A smoothed version of the solution would show the usual Sverdrup interior flow $u_R = -1/y_N$ as well as boundary layers near $y = 0$ and $y = y_N$.

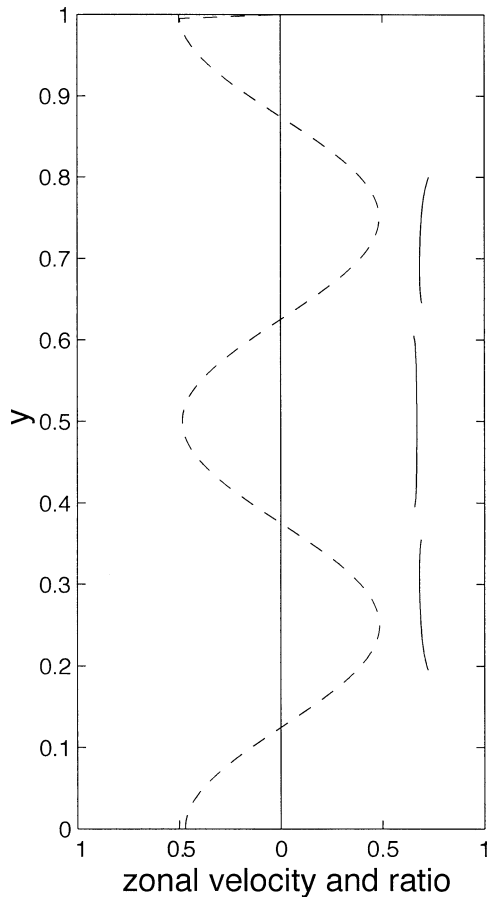In order to explore the dynamics of the fluctuations

FIG. 10. The zonal velocity (dashed line) from the shallow-water model with a sinusoidal wind stress curl [see (3.9)] and no ridge. The solid line is the ratio of the zonal velocity for a case with a porous ridge located between $y = 0.2$ and 0.8 [$p = 0.2$, $(l/\lambda) = 0.15$] and the case with no ridge. (The ratio is not plotted in regions where the zonal velocity is near zero.) The ratio is nearly constant, and close to the theoretical value of 0.53 for these parameters.
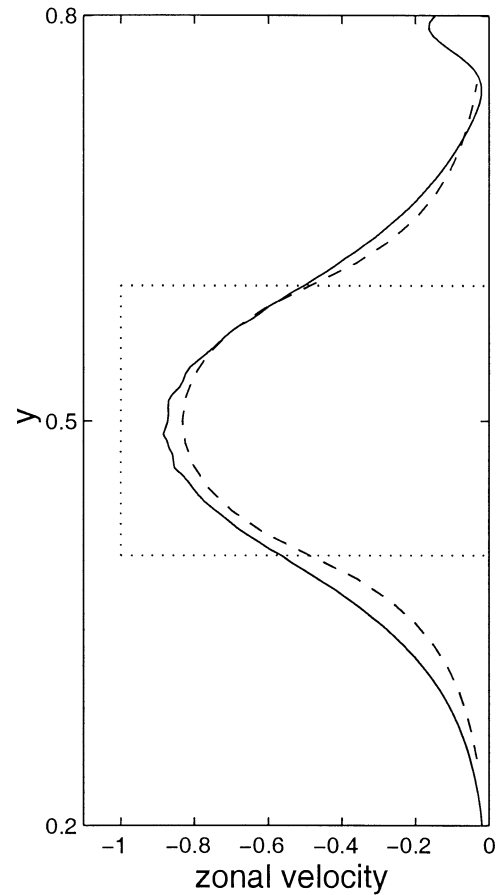

FIG. 11. The zonal velocity to the west of the porous ridge (located between $y = 0.2$ and $y = 0.8$) for a case with localized wind stress curl between $y = 0.4$ and $y = 0.6$ (indicated by the dotted lines), normalized by the zonal Sverdrup velocity in the absence of any islands. Solid line: shallow-water model; dashed line: theory [from (3.13)].

more thoroughly, we attempt to find an asymptotic solution to (3.18) for the interior flow only. By trial and error, it can be shown that the appropriate expansion takes the form

$$T = -\frac{y}{y_N} + \varepsilon^3 \hat{T}\left(\frac{y}{\varepsilon}\right).$$

Since the nondimensional distance y_N is typically large, $1/y_N$ is regarded as $O(\varepsilon)$. Substitution into (3.18) leads to the lowest-order problem

$$\hat{T}'' + \frac{1}{\varepsilon y_N \overline{p}} \hat{p}' = 0. \qquad (3.19)$$

Both terms are associated with dissipation [the first two terms in (3.18)], and thus the lowest-order balance involves a requirement of net zero dissipation about each island. The solution to (3.19) can be written as

$$\hat{T} = \frac{-1}{\varepsilon y_N \overline{p}} \int^{y/\varepsilon} \hat{p}(\eta) \, d\eta + c_1 \frac{y}{\varepsilon} + c_2.$$

For the interior region (away from $y = 0$ and $y = y_N$) we choose $c_1 = c_2 = 0$ since there is no reason to expect a linearly growing or constant offset as a response to the fluctuating porosity. The full zonal velocity associated with this solution is given by

$$\frac{u_R(y)}{u_S(-L, y)} = \frac{-(y_N \overline{p})^{-1}[1 + \varepsilon \hat{p}(\eta)]}{-(y_N)^{-1}} = \frac{p}{\overline{p}}. \qquad (3.20)$$

As with the example involving the discontinuity in p, the westward Sverdrup velocity through the ridge is enhanced where p is higher than average ($\hat{p} > 0$) and retarded where p is lower than average. Note that the velocity in the straits u_R/p is constant. When applied with the settings used to produce the numerical solution (Fig. 13), (3.20) yields an approximation (the dashed curve) that is very close.
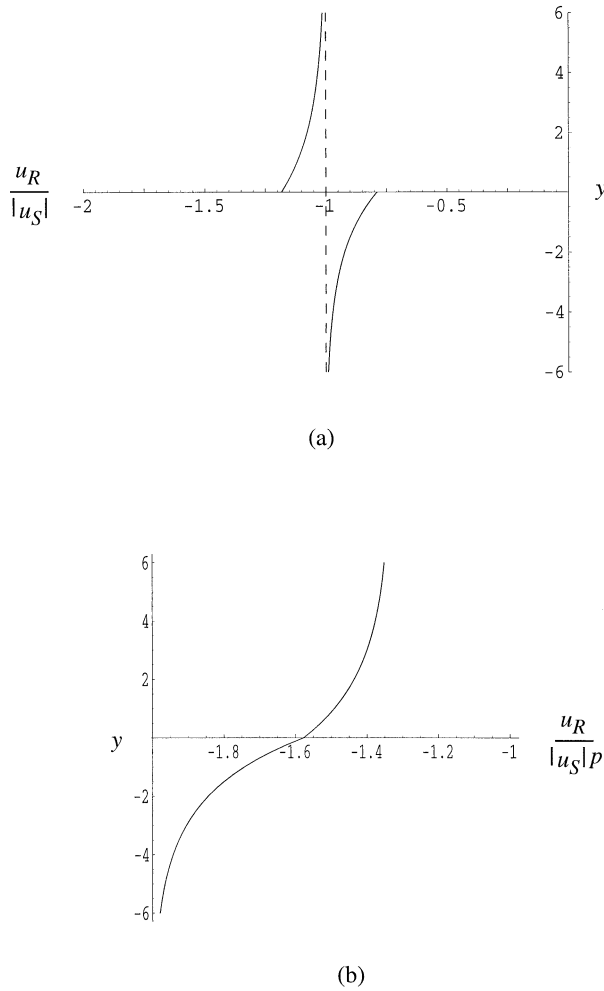
(a)

(b)

FIG. 12. The zonal velocity produced at the west edge of the ridge by a discontinuity in porosity. The porosity changes from a constant value $p = 0.5$ to $p = 0.75$ at $y = 0$. (a) The microscopically averaged velocity shows a discontinuity, whereas (b) the actual velocity in the straits is continuous. Note that y has been scaled by $(\delta_s L)^{1/2}$.

4. Formulation for a multilayer, quasigeostrophic system

If the layer in question is part of a steady, multilayer, quasigeostrophic model, then it is not too difficult to show that flow through the ridge interior remains governed by (3.2) with a few minor modifications. One must continue to assume that the islands and straits within the ridge are rectangular and that the sidewalls are vertical over the depth of contact with the layer in question. The distribution of gaps and islands, and therefore the porosity and ridge width, may change from one layer to the next.

Consider layer j, which has undisturbed thickness $D^{(j)}$ and actual thickness $D^{(j)} + d^{(j)}(x, y)$. Under the assumption of quasigeostrophy, $d^{(j)} \ll D^{(j)}$, a feature crucial to what happens next. As shown by Pedlosky et al. [(1997), Eq. (A.3)] the linearized circulation integral analogous to our (2.4) for island n and within layer j is
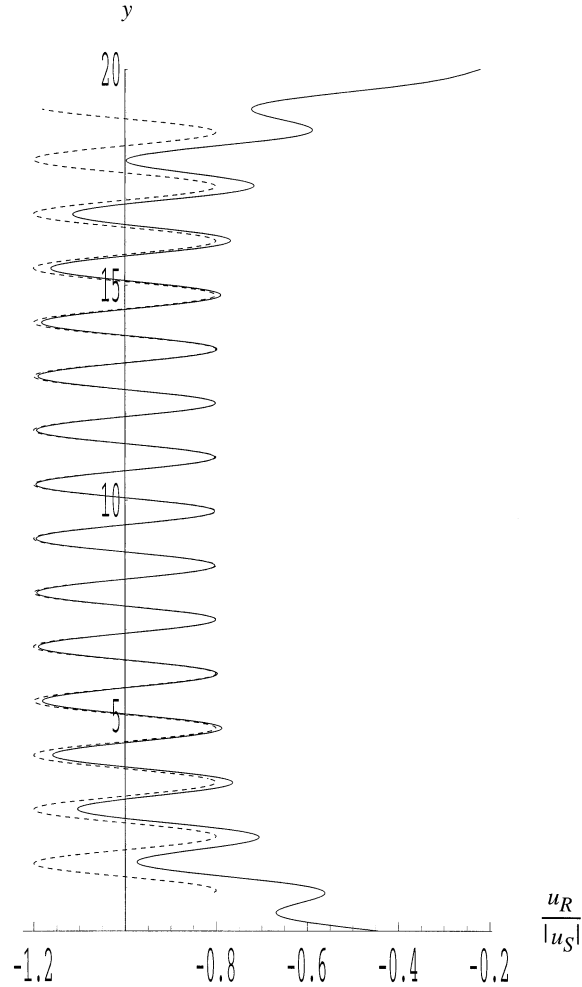

FIG. 13. The dashed curve gives the theoretical zonal velocity [see (3.20)] at the west edge of the ridge for the interior latitude band of the ridge when the porosity varies rapidly [$p = 0.5 + 0.1 \sin(y/0.2)$] and when the wind stress curl varies linearly in y. The solid curve corresponds to a numerical solution of (3.18) that satisfies the boundary conditions at the north and south tips of the ridge ($y = 0$ and $y = y_N = 20$). Note that y has been scaled by $(\delta_s L)^{1/2}$ $L = 0.5$ and $\alpha = 0.95$.

$$\beta \delta_n^{(j)} T_n^{(j)} = \oint_{\Gamma_n^{(j)}} [\mathbf{F}^{(j)} - D_f \mathbf{u}^{(j)}] \cdot \mathbf{t} \, ds. \quad (4.1)$$

Here $\mathbf{F}^{(j)}$ is a generalized momentum forcing term analogous to τ/ρ in the previous case. This forcing would include the vertical transport of horizontal momentum resulting from entrainment of fluid from the overlying and underlying layer. If dissipation about $\Gamma_n^{(j)}$ term occurs primarily within the straits, then

$$\oint_{\Gamma_n^{(j)}} D_f \mathbf{u}^{(j)} \cdot \mathbf{t} \, ds$$

$$\cong D_f \left[\int_{-L_{n-1}^{(j)}}^0 u_{n-1}^{(j)} \, dx - \int_{-L_n^{(j)}}^0 u_n^{(j)} \, dx \right]$$

$$
= D_f \left\{ \int_{-L_{n-1}^{(j)}}^{0} \frac{Q_{n-1}^{(j)}}{[D^{(j)} + d_{n-1}^{(j)}]\Delta_{n-1}^{(j)}} \, dx \right.
$$

$$
\left. - \int_{-L_n^{(j)}}^{0} \frac{Q_n^{(j)}}{[D^{(j)} + d_n^{(j)}]\Delta_n^{(j)}} \, dx \right\}
$$

$$
\cong D_f L_n^{(j)} \left[\frac{Q_{n-1}^{(j)}}{D^{(j)}\Delta_{n-1}^{(j)}} - \frac{Q_n^{(j)}}{D^{(j)}\Delta_n^{(j)}} \right]
$$

$$
- D_f \left\{ \int_{-L_n^{(j)}}^{0} \left[\frac{Q_{n-1}^{(j)}}{D^{(j)}\Delta_{n-1}^{(j)}} \frac{d_{n-1}^{(j)}}{D^{(j)}} - \frac{Q_n^{(j)}}{D^{(j)}\Delta_n^{(j)}} \frac{d_n^{(j)}}{D^{(j)}} \right] dx \right\}.
$$

The continuity equation has been used to derive the second line and, in doing so, it has been acknowledged that the layer depth may vary along the length of each strait. The layer depth may also vary from strait to strait. Both types of variations are contained in the second integral on the final line but this term is smaller than the first term by a factor $d^{(j)}/D^{(j)} \ll 1$. Neglect of this term means that the dissipation integral is identical to the result (2.6) from the barotropic case. The steps leading to (2.10) are the same as before, and therefore the transport to the east of the ridge within layer j is given by

$$
\frac{d}{dy} \left[\frac{1}{p^{(j)}(y)} \frac{dT^{(j)}}{dy} \right] - \frac{[1 - p^{(j)}(y)]}{\delta_s L^{(j)}(y)} T^{(j)}
$$

$$
= -\frac{[1 - p^{(j)}(y)]}{\delta_s L^{(j)}(y)} T_I^{(j)}(y), \tag{4.2}
$$

where

$$
T_I^{(j)}(y) = \lim_{\delta_n^{(j)} \to 0} \frac{\oint_{\Gamma_n^{(j)}} \mathbf{F}^{(j)} \cdot \mathbf{t} \, ds}{\beta \delta_n^{(j)}}.
$$

It is not the case, however, that the boundary conditions for (4.2) will remain the same as in the barotropic case. If the north or south end of the ridge is free, the boundary condition will depend on the dissipation along that edge. The frictional boundary layer that exists there may be more complicated than the diffusive layer considered in the barotropic model. The precise scaling will depend on the relative size of the various internal deformation radii and other length scales that arise in the layer model. The correct condition will depend on the model in question.

5. Discussion

We have developed a porous-medium theory for barotropic flow through complex ridges and archipelagos. The governing field equation also is valid for quasigeostrophic, layered flow (though the boundary conditions may differ). The dynamical underpinning of the theory is the circulation integral over a "Godfrey" contour for each of the bumps or islands that compose the ridge. Each integral can be expressed as a difference equation for the meridional transport to the east of the boundary. When the meridional dimensions of the islands and separating gaps vary gradually and their values are made infinitesimal, the difference equations reduce to a second-order differential equation (2.10) for the meridional transport. The divergence of the transport gives the zonal transport through the ridge as a function of its porosity $p(y)$ and zonal width $L(y)$. The theory assumes that the gaps separating the islands are orientated zonally, in the manner of fracture zones in the Mid-Atlantic Ridge, that the primary source of dissipation in the circulation integral is bottom friction acting in the gaps, that the flow is steady and linear, and that the flow in each gap becomes uniform as the gap thickness approaches zero.

Analytical examples with verifying numerical simulations have yielded some interesting and unintuitive results concerning the physics of flow through the ridge. For example, it can be shown that the throughflow is associated with the natural length scale $l = [\delta_s L/p(1 - p)]^{1/2}$, a measure of the meridional extent over which irregularities in the impinging flow are spread as this flow is absorbed. Although it is not surprising that l should tend toward infinity for a solid ridge ($p \to 0$), it is curious that the same behavior occurs when the ridge becomes highly porous ($p \to 1$). As explained in section 2, the latter result stems from the disproportionally high dissipation that would result around each island if the islands were thin in comparison with the gap widths and l remained finite. (This behavior does occur in the numerical model, though technical problems make it difficult to explore p values more than about 0.8.)

If the ridge porosity is uniform the ability of the ridge to block or divert an impinging zonal flow with meridional scale λ depends on l/λ. If the impinging flow is broad ($l/\lambda \ll 1$) then it will be unimpeded by the ridge. As was shown by the example in section 3b zonal velocity at the west edge of the ridge is the same as if the ridge were absent, though other effects occur within a distance l of the ends of the ridge. If $l/\lambda \geq O(1)$ the flow must spread meridionally before it can pass through the obstacle (section 3d). If the impinging zonal flow consists of alternating bands (section 3c), the spreading effect leads to cancellation of the eastward and westward flows. For the case of very narrow bands ($l/\lambda \gg 1$) the cancellation is nearly complete and very little fluid passes through the ridge.

The effect of variable porosity introduces additional length scales, and when these are small in comparison with l and λ the throughflow can described by an asymptotic theory (section 3e). The value of p is assumed to undergo weak but rapid fluctuations about a mean. A solution for sinusoidal fluctuations and a uniform impinging flow shows throughflow enhancement in areas of higher p and impedance in regions of low p. It is not known whether the limit of rapid but smooth

fluctuations in p reflects the physics of cases for which the spatial dimensions of the topography vary abruptly from one "island" or gap to the next. As suggested by Fig. 1, abrupt and perhaps random variations may be more realistic than the smooth variations assumed in the derivation of our governing differential equation. However, it should be possible to explore the dynamics associated with abrupt variations by iterating (2.7).

Another allowance one could hope to add is for large variations in layer thickness through the gaps in the ridge. Such variations occur when fluid spills from one basin to the next, giving rise to hydraulic effects and form drag.

APPENDIX A

The Boundary Layers on the North and South Coasts of the Ridge

Under the assumption that the wind stress curl is uniform in x, analytical solutions for the velocity in the diffusive boundary layers along the north and south coasts of the porous ridge can be found [see Pedlosky et al. (1997), Eq. (2.34)]. The corresponding expression for the zonal velocity in the boundary layer on the south edge is

$$\frac{u}{|u_S|} = \frac{-(x - \Delta_E)y_N \frac{\partial}{\partial y}\, \mathrm{curl}\left(\frac{\tau}{\rho}\right)_{y=0}}{(L + \Delta_E)\left|\mathrm{curl}\left(\frac{\tau}{\rho}\right)_{y_N}\right|} + \frac{y_N}{(-\pi x \delta_S)^{1/2}}\left[T(0) - \frac{\Delta_E\, \mathrm{curl}\left(\frac{\tau}{\rho}\right)_{y=0}}{(L + \Delta_E)\left|\mathrm{curl}\left(\frac{\tau}{\rho}\right)_{y_N}\right|}\right]e^{y^2/(4x\delta_S)}$$

$$+ \frac{y_N L^{1/2}\, \mathrm{curl}\left(\frac{\tau}{\rho}\right)_{y=0}}{(L + \Delta_E)\left|\mathrm{curl}\left(\frac{\tau}{\rho}\right)_{y_N}\right|}\left\{\frac{-y}{(\delta_S L)^{1/2}}\, \mathrm{erfc}\left[\frac{y}{2(x\delta_S)^{1/2}}\right] - 2\left(\frac{-x}{\pi}\right)^{1/2} e^{y^2/(4x\delta_S)}\right\} \qquad (-L \le x < 0, \, y \le 0),$$

where $T^*(y)$ is the dimensional transport to the east of the porous boundary,

$$T(y) = T^*(y)\beta/[(L + \Delta_E)|\mathrm{curl}(\tau/\rho)_{y_N}|]$$

is the dimensionless counterpart (scaled with the total Sverdrup transport between the northwest corner of the ridge and the eastern basin boundary), and all other quantities may be regarded as dimensional. The scaling factor $|u_S|$ is the magnitude of the Sverdrup velocity at the west edge of the island that would be produced when the wind stress curl varies uniformly from zero at $y = y_S$ to value $\mathrm{curl}(\tau/\rho)_{y_N}$ at y_N.

The corresponding expression for u in the boundary layer along the north ridge can be obtained from the above expression by reversing the sign of the second and third terms on the right-hand side and replacing $-y$ by $(y - y_N)$ and $T(0)$ by $T(y_N)$.

APPENDIX B

The Shallow-Water Numerical Model

The nondimensional shallow-water momentum equations may be written as

$$R(\mathbf{v}_t + \mathbf{v}\nabla\mathbf{v}) + (1 + \beta y)\mathbf{k} \times \mathbf{v}$$
$$= -\nabla h - \mathbf{C}\mathbf{v} + \beta\boldsymbol{\tau}/H(1 + B^{-1}Rh),$$

where $\mathbf{v}$ is the horizontal velocity vector, h is the layer thickness, and $\boldsymbol{\tau}$ is the wind stress. The continuity equation is written as

$$h_t + R^{-1}B\nabla \cdot \mathbf{v} + \nabla \cdot (\mathbf{v}h) = 0.$$

The variables have been nondimensionalized by a velocity scale U, a horizontal length scale L, and a vertical length scale H. The deviation of the layer thickness h from the motionless value is scaled as f_0UL/g'. The Coriois parameter is assumed to vary linearly with latitude as $f = f_0 + \beta^*y$, where f_0 is the Coriolis parameter at the central latitude of the domain and β^* is the dimensional variation of the Coriolis parameter with latitude. The reduced gravity between the moving layer and the deep ocean is g'. Time has been nondimensionalized with the advective timescale L/U and the wind stress is nondimensionalized by $\rho_0U\beta^*L$. This scaling results in several nondimensional numbers. The Rossby number $R = U/fL$ is a measure of the strength

of the nonlinear terms. The drag coefficient $C = \beta^* \delta_s / f_0$, where δ_s is the Stommel boundary layer width, measures the strength of dissipation. The variation of the Coriolis parameter over the meridional scale of the domain is measured by $\beta = \beta^* L / f_0$. The Burger number $B = (L_d / L)^2$, where $L_d = \sqrt{g'h / f_0}$ is the internal deformation radius. The model is integrated on a staggered C grid and the equations are solved using a second-order centered finite-difference scheme. Time stepping is achieved with a third-order-accurate Adams–Bashforth scheme. The lateral boundary conditions are no slip and no normal flow. The model domain is a square with nondimensional size 1.0. The resolution is 200×200, so that the (nondimensional) grid resolution is 0.005. The model calculations are run with $\Delta = 0.005$ and the island width $L = 0.1$. The calculations are essentially linear with $R = 0.001$. The stratification is such that the deformation radius is equal to the basin dimension, $B = 1$. The variation in the Coriolis parameter is important over the meridional extent of the basin with $\beta = 0.4$.

The porous ridge extends from $x = 0.45$ to $x = 0.55$ and from $y = 0.2$ to $y = 0.8$, giving $y_N - y_S = 0.6$ (e.g., Fig. 7). Unless stated otherwise, the ridge is made up of 24 discrete islands each of meridional dimension $\Delta = 0.02$ and the porosity $p = 0.2$ so that the gap widths are $\delta = 0.005$. The model is forced by a steady, zonal wind stress applied as a force in the momentum equations. The forcing is confined to the region to the east of the western edge of the islands ($x = 0.45$) and will be varied for comparison with the theory. The wind stress curl is kept constant to the north (south) of the ridge at the same value as at the northern (southern) tip of the ridge. This allows the meridional transport to continue smoothly approaching and departing the ridge system, and for the effects of the northern and southern boundaries of the model to be isolated from the region of interest. The model is run until steady state is achieved.

REFERENCES

Faller, A. J., 1960: Further examples of stationary planetary flow patterns in bounded basins. *Tellus,* **12,** 159–171.

Godfrey, J. S., 1989: A Sverdrup model of the depth-integrated flow from the world ocean allowing for island circulations. *Geophys. Astrophys. Fluid Dyn.,* **45,** 89–112.

Pedlosky, J., 1968: An overlooked aspect of the wind-driven ocean circulation. *J. Fluid Mech.,* **32,** 809–821.

——, L. J. Pratt, M. A. Spall, and K. R. Helfrich, 1997: Circulation around islands and ridges. *J. Mar. Res.,* **55,** 1199–1251.

Pratt, L. J., and J. Pedlosky, 1998: Barotropic circulation around islands with friction. *J. Phys. Oceanogr.,* **28,** 2148–2162.

Smith, W. H. F., and D. T. Sandwell, 1997: Global sea floor topography from satellite altimetry and ship deep soundings. *Science,* **277,** 1956–1962.

Wajsowicz, R. C., 1993a: The circulation of the depth-integrated flow around an island with applications to the Indonesian Throughflow. *J. Phys. Oceanogr.,* **23,** 1470–1484.

——, 1993b: A simple model of the Indonesian Throughflow and its composition. *J. Phys. Oceanogr.,* **23,** 2683–2703.

——, 2002: A modified Sverdrup model of the Atlantic and Caribbean circulation. *J. Phys. Oceanogr.,* **32,** 973–993.